phys. stat. sol. (b) **208**, 257 (1998)

Subject classification: 78.30.Er; 63.20.Dj; S1

Raman Scattering in Os: Nonadiabatic Renormalization of the Optical Phonon Self-Energies

YU. S. PONOSOV (a), G. A. BOLOTIN (a), C. THOMSEN (b), and M. CARDONA (c)

(a) Institute for Metal Physics UD RAS, S. Kovalevskoi 18, 620219 Ekaterinburg, Russia

(b) Institut für Festkörperphysik, Technische Universität Berlin, Hardenbergstr. 36, D-10623 Berlin, Germany

(c) Max-Planck Institut für Festkörperforschung, Heisenbergstr. 1, D-70569 Stuttgart, Germany

(Received September 17, 1997)

The wave vector dependence of the E_{2g} optical phonon frequencies and linewidths in the hexagonal close-packed metal, osmium, was studied at 10 K. A strong anisotropic dispersion, as well as damping thresholds, were observed for two transverse branches in the high-symmetry directions of the Brillouin zone around a phonon wave vector magnitude of 10^6 cm^{-1}. Simultaneously, a continuum was found in the Raman spectra, presumably of electronic nature, whose **q**-dependence correlates with that the phonon self-energies. Numerical simulations of the electronic Raman response in terms of an intraband mechanism were performed with a model energy-band spectrum reproducing the main features of the Fermi surface anisotropy of Os. A large discrepancy was found between the calculated and the measured anisotropy of the electronic scattering with respect to momentum direction and polarization configuration. The possible assignment to a contribution of resonant terms to the Raman vertex is discussed.

1. Introduction

A great deal of experimental and theoretical effort [1 to 8] has been devoted during the last few years to understand the origin of the electronic excitations observed by Raman scattering in d-metal-based superconductors, and in particular HTSCs, and the modification of their coupling with phonons at the superconducting transition [9 to 11]. In most published works, the Raman vertex for light scattering by electrons is assumed, for simplicity, to be related to the curvature of the Fermi surface (FS) in spite of the resonant character of this phenomenon in metals: A consideration of the resonant vertices would require extended energy band structure calculations [12]. In addition, the response of the electronic system of these metals is often discussed within the collision-limited regime [10] because of the large scattering rates involved. Nevertheless, some experimental evidence of the dependence of phonon self-energy changes on the incident laser energy in $YBa_2Cu_3O_7$ [13] and previously in p-Ge [14] has been interpreted assuming the **k**-vector of an electron to be a good quantum number. The investigations of spatial dispersion effects in the electron–phonon excitations of clean metals with long mean free path l have been so far limited by the observation of anomalous E_{2g} phonon damping in a number of hexagonal close-packed (h.c.p.) metals [5] where different phonon broadenings were observed for different phonon wave vector directions at low temperatures.

The theory of the optical phonon renormalization by intraband electronic excitations in the normal state of a metal [16] predicts phonon hardening and no channels for dampling in the nonadiabatic region $q < \omega_0/v_F$ (ω_0 is the phonon frequency, v_F the Fermi velocity) for the **k**-conserving case. Together with a strong phonon dispersion and Landau damping for $\omega_0 < qv_F$, one should be able to observe in Raman scattering a continuum of electronic excitations interacting with the phonons. Its frequency, wave vector and polarization dependences may give important information on the structure of the FS [17].

q-dependent effects in phonon self-energy and electronic Raman scattering have also been treated as arising from diffusion terms in both pure and dirty normal metals [18 to 22]. However, clear evidence of wave vector dependence in Raman scattering by electrons in a normal metal has, to our knowledge, not yet been reported.

In the present work we discuss the results of a detailed Raman study of the low temperature **q**-dependent phonon self-energy and electronic light scattering in the transition metal osmium. The dispersion of the optical phonon branches around the E_{2g} zone-center mode is shown to be rather anisotropic for different high-symmetry directions of the Brillouin zone and to be accompanied by **q**-dependent phonon linewidths. The observation of the electronic Raman continuum with a striking **q**-dependence implies a strong interaction between the electronic and vibrational excitations under study. We carried out model calculations of the intraband electronic Raman continua taking into account the anisotropy of the FS of Os, which is presumed to determine the frequency dependence of the spectra for different **q**-directions and the anisotropy of the phonon self-energy. We compare the results of these calculations with the corresponding experimental data.

2. Experimental Details

Osmium crystallizes in the h.c.p. structure with two atoms per unit cell (space group D_{6h}^4). Its point group D_{6h} leads to Raman activity for scattering configurations which correspond to the irreducible representations

$$A_{1g} + E_{1g} + E_{2g} \tag{1}$$

having following forms of the Raman tensors:

$$A_{1g} = \begin{pmatrix} a & 0 & 0 \\ 0 & a & 0 \\ 0 & 0 & b \end{pmatrix}, \qquad E_{1g,1} = \begin{pmatrix} 0 & 0 & 0 \\ 0 & 0 & d \\ 0 & e & 0 \end{pmatrix}, \qquad E_{1g,2} = \begin{pmatrix} 0 & 0 & d \\ 0 & 0 & 0 \\ e & 0 & 0 \end{pmatrix},$$

$$E_{2g,1} = \begin{pmatrix} 0 & f & 0 \\ f & 0 & 0 \\ 0 & 0 & 0 \end{pmatrix}, \qquad E_{2g,2} = \begin{pmatrix} f & 0 & 0 \\ 0 & -f & 0 \\ 0 & 0 & 0 \end{pmatrix}. \tag{2}$$

Among the optical phonons only those of E_{2g} symmetry are Raman active (the B_{1g} mode is silent). For the doubly degenerate E_{2g} phonons the two sublattices make opposite displacements in the x- and y-directions of the basal plane. The $E_{2g,1}$ matrix corresponds to the vibration along the y-axis and the $E_{2g,2}$ tensor to that in the x-direction. Therefore, the phonons with small but finite wave vector along the $c(z)$-axis are transverse but transverse and longitudinal phonons (containing the full-symmetric component) may be both observed by Raman spectroscopy if the investigated wave vectors lie in the basal plane.

Three Os samples with scattering surface orientations (0001), $(10\bar{1}0)$ and $(1\bar{2}10)$ were cut from the same crystal, having a residual resistance ratio (RRR) = 1600, and then prepared by electropolishing in order to obtain strain-free surfaces. The lines of Ar^+, a Kr^+ and a Ti:sapphire laser with powers up to 50 mW, focused to a spot of $30 \times 30\,\mu m^2$ in near backscattering geometry, were used for excitation. Variation of the incident photon energy (1.5 to 2.7 eV) provided the possibility to change the magnitude of the probed wave vector by nearly a factor of three, from (6 to 18)$\times 10^5\,cm^{-1}$. No local heating effects were found during measurements with different laser powers. The data were taken at temperatures ranging from 10 to 300 K using a close-cycle helium refrigerator; only low-temperature results will be presented in this paper. The scattered-light spectra were analyzed with a Dilor *XY* Raman spectrometer using a multichannel nitrogen-cooled CCD detector.

3. Experimental Results

In Fig. 1 we present Raman spectra of Os measured at 10 K with different laser energies (1.6 to 2.5 eV) for two wave vector directions and for polarizations xx/yy and xy corresponding to $A_{1g} + E_{2g}$ and pure E_{2g} symmetry, respectively. These spectra show the E_{2g} 170 cm^{-1} phonon line superimposed on a background, presumed to be electronic, whose peak frequency hardens with increasing incident energy and momentum transfer **q** (estimated from optical data [23]). As a rule, the energy of the peak in the electronic continuum for **q** along [0001] is higher by 15 to 20% than that in the perpendicular configuration. This ratio of the energies of the continua and that of the corresponding scattering intensities for different polarizations shows only small changes in the range of the exciting energies (i.e., probed crystal momenta) used (see Fig. 2). The only exception is a crossing of the continuum energies near 1.8 eV where the peak frequency for **q** in the basal plane becomes marginally larger (Figs. 1 and 2). The spectra for two in-plane **q**-directions differ less from each other, e.g., in intensity and frequency dependence, than from that for **q** along the *c*-axis. The latter also shows a more rapid growth at low frequencies. Spectra taken with polarized light and with an analyzer in front of the spectrometer (see Fig. 1) demonstrate that electronic scattering with similar lineshapes is observed for both A_{1g} and E_{2g} scattering geometries.

The scattering spectra of the two E_{2g} optical phonons, degenerate at the zone center, also show significant wave vector dependence in their peak energies and linewidths. In order to obtain the corresponding phonon parameters, the measured spectra were fitted with either Lorentz or Fano expressions [24] after subtraction of a smooth background (presumed to be electronic) estimated over a frequency range about twenty times wider than the phonon linewidths. The fitting parameters so obtained and their dispersion are shown in Fig. 3. We have not plotted the Fano asymmetry parameters because they contain little information within the error given by the fit. Their magnitude is always larger than four (with either + or − signs) a fact which corresponds to the moderate asymmetry of the observed phonon profiles. The strong frequency dispersion found for the $[1\bar{2}10]$ and [0001] **q**- directions is in sharp contrast to the much weaker one [within experimental error bars) observed for **q** along $[10\bar{1}0]$. The derivative $d\omega/dq$ evaluated at low frequencies for **q** along the $[1\bar{2}10]$ direction is larger than 10^6 cm/s, i.e. is close to the Fermi velocities of the electrons. To our knowledge, there is no previous observation of such a strong spatial dispersion (or

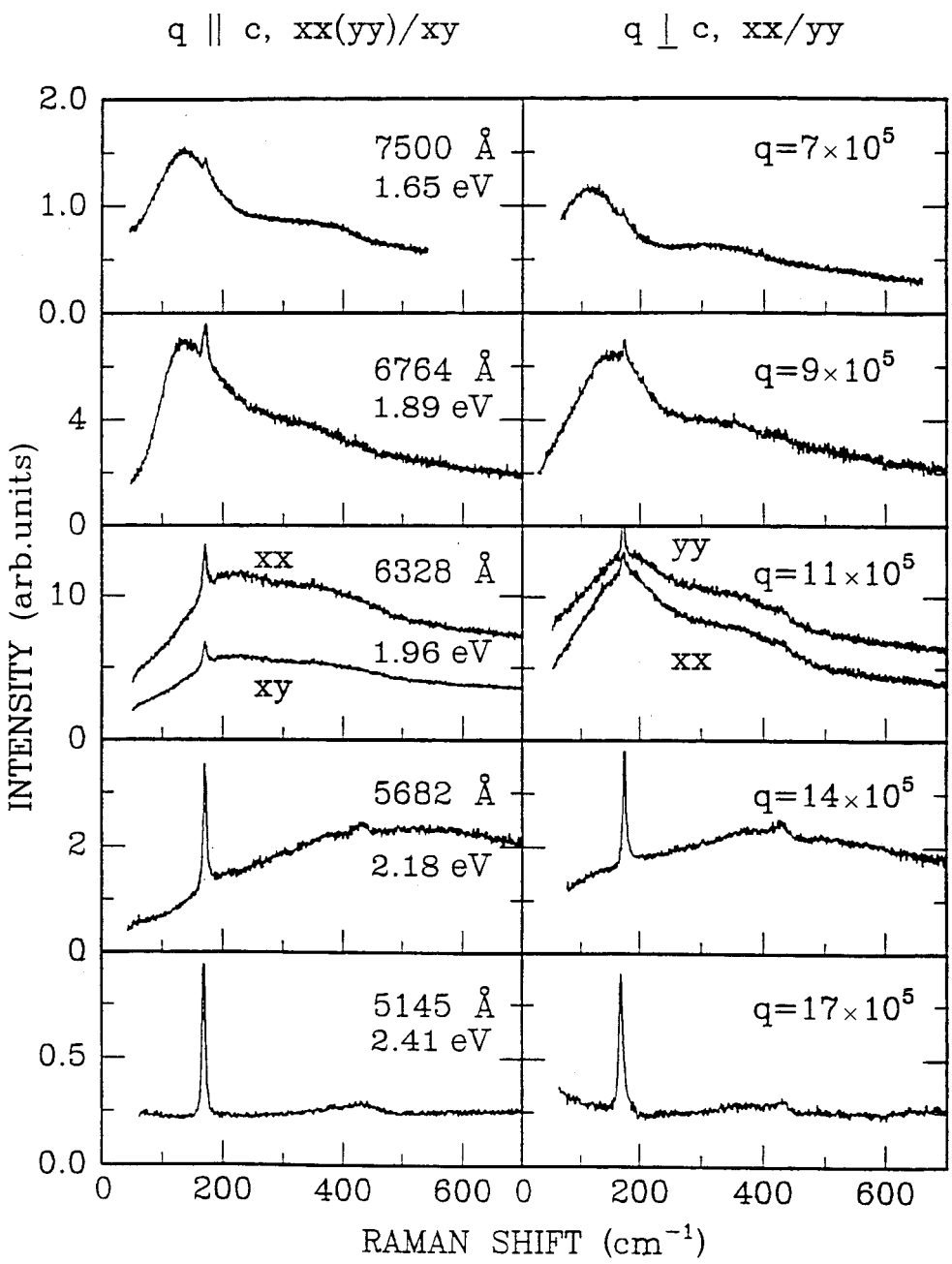

Fig. 1. Raman spectra measured at 10 K in the backscattering configuration for different crystal planes and a number of exciting energies and polarizations yy/xx and xy ($\lambda = 6328$ Å). The weak bands seen in the experimental spectra near 400 cm^{-1} are due to scattering by two phonons. The wave vector magnitudes (in cm^{-1}) were estimated with optical data [23]. The relative intensities are presented as measured, no corrections for light transmission and absorption, as well as spectrometer response were performed

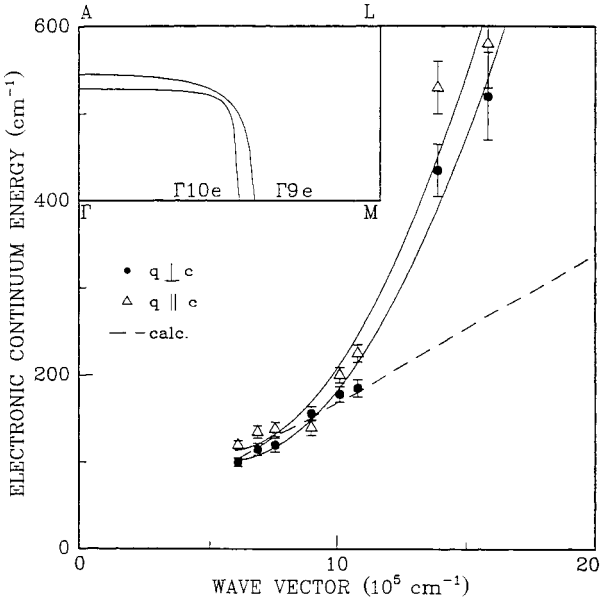

Fig. 2. Measured (the solid lines through the points are guides to the eye) and calculated dependences of the peak energy for in-plane **q** in the electronic scattering continuum on the magnitude of the wave vector (dashed line; only the band parameter E_1 was adjusted, see text). Insert: section of model Fermi surface sheets Γ9e and Γ10e used in the calculations, as obtained with Eq. (9)

q-dispersion) of an even parity phonon near the zone center. The dependence of the phonon width on wave vector for $\mathbf{q} \parallel [1\bar{2}10]$ has a clear maximum near $q \approx 1.1 \times 10^6\,\mathrm{cm}^{-1}$, which approximately coincides with the wave vector of the frequency anomaly (point of maximum dispersion). For $\mathbf{q} \parallel [0001]$ the maximum occurs at lower q-values, consistent with a similar trend in the frequency anomaly. The optical phonons with $\mathbf{q} \parallel [10\bar{1}0]$ have the weakest dispersion and give only a small indication of a maximum in the FWHM (Fig. 3). Since the values extracted for the phonon parameters are strongly dependent on **q**, they may still be affected by wave vector "smearing" which must result from the finite penetration depth of the ligth. Nevertheless, the data presented here show that anomalies in phonon self-energies exist in the q-region near $10^6\,\mathrm{cm}^{-1}$. Notably, these anomalies occur at the excitation energies where the peak of the electronic scattering moves through the phonon energy (Fig. 1). This suggests that the anomalies are related to some kind of interaction between the phonons and the observed electronic excitation continuum and provides an opportunity to discuss both effects within a consistent framework in an effort to understand the origin of the spatial dispersion of these striking phenomena.

4. Numerical Simulations and Comparison to Experiment

The first type of excitations we discuss are intraband electronic excitations, which would give rise to both, nonadiabatic phonon renormalization [16] and Raman scattering by conduction electrons in metals with anisotropics FS [17]. In this case, the phonon self-energy and the electronic Raman continuum must be obtained through integrals of the electronic response function over FS sheets, weighted either by matrix elements of the electron–phonon interaction (in the case of phonon self-energy) or by the Raman vertex for electronic scattering. In this approach one takes the response function of

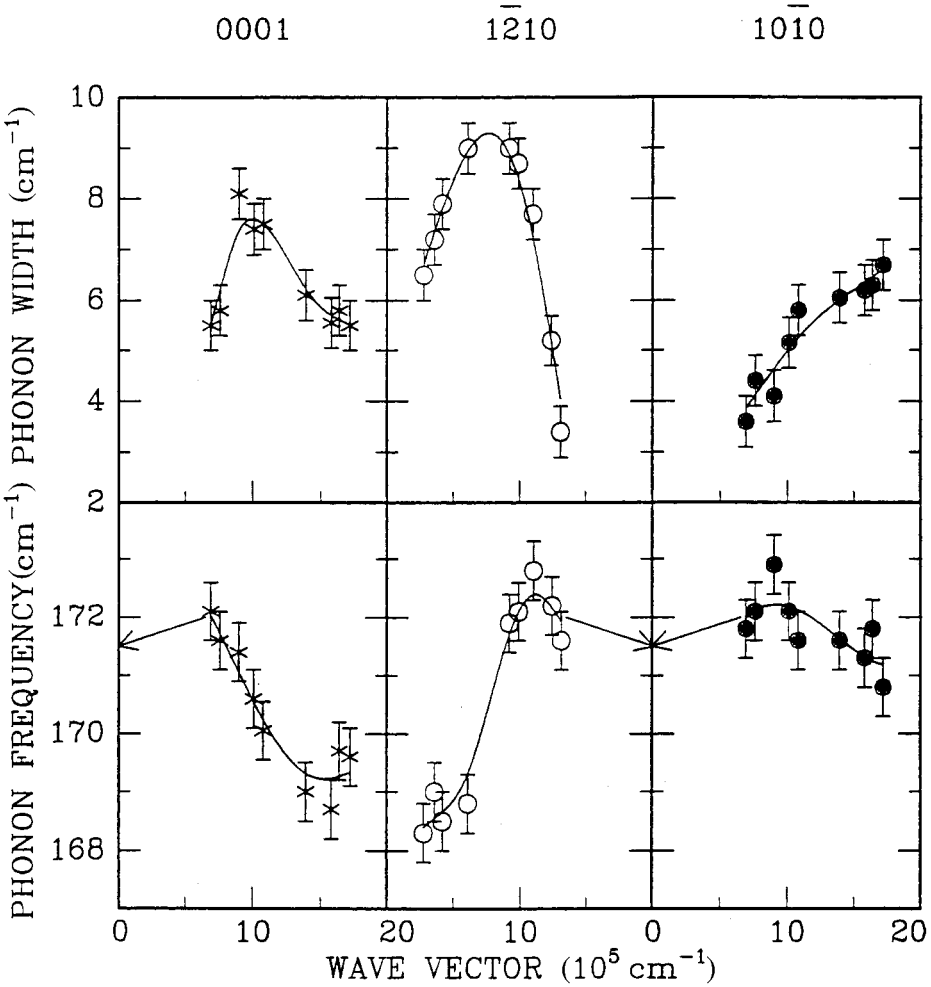

Fig. 3. Frequencies and linewidths of the E_{2g} phonon extracted from experimental data (circles and crosses represent experimental points, the solid lines are guides to the eye) as a function of wave vector magnitude and direction. The error bars were determined from the scatter of repeated measurements performed on the same sample

noninteracting electrons

$$\frac{qv}{qv-\omega-i\Gamma}, \tag{3}$$

where Γ is the relaxation frequency of electrons, since the polarization operator is in the regime of weak scattering. The formal analogy existing between the two processes phonon self-energy and electronic scattering cross-section, [10] may be the reason of the correlation observed in the dependence of both effects on **q**.

Another possible mechanism providing **q**-dependent effects is a diffusion term Dq^2 in the polarization operator within the collision limited regime [10, 22]. The diffusion term

Dq^2 is proportional to

$$Dq^2 \sim \left(\frac{qv}{\omega + i\Gamma}\right)^2 \tag{4}$$

and becomes important in the limit $\omega \ll \Gamma$ and $ql \ll 1$: it can give a **q**-dependent contribution to electronic Raman continuum and phonon self-energies [10, 18, 20, 22] even in the case of a pure metal [18]. This happens in a metal because of nonconservation of transferred momentum in the penetration depth of the radiation, leading to the contribution of small wave vectors to electronic scattering. The values $\Gamma \approx 1\,\mathrm{cm}^{-1}$ and $ql \approx 1000$ were estimated for the high-purity samples under investigation (they correspond to the peak in the distribution of the transferred wave vector at the laser energies used in our experiments). This means that a diffusion term may provide a sizeable contribution only at very low frequencies $\omega < 1\,\mathrm{cm}^{-1}$ and wave vector $q < 10^3\,\mathrm{cm}^{-1}$. Keeping in mind that in such case only a small part of the total wave vector distribution is active and that the spectra were measured as a rule beginning at $50\,\mathrm{cm}^{-1}$, we should not attribute the observed **q**-dependent effects to a diffusion mechanism and will not take it into account in the following simulations.

Close attention, however, should be paid to the role of the **k**-dependences of both vertices which is not obvious when the response function of the noninteracting electrons is calculated. The theory of the light scattering by conduction electrons in a metal with an anisotropic FS relates the Raman vertex to the FS curvature [17]. This provides a simple way to reach some conclusions about the origin of the electronic excitations under study by comparing the experimental data to the simulations for the model FSs. Hence we carried out calculations of the **q**-dependent electronic Raman spectra using model energy bands which reproduce the anisotropy of the Os Fermi surface. The dependence of the electronic scattering cross-section on frequency ω and wave vector **q** is determined by the generalized susceptibility of the conduction electrons [17]

$$W_{\alpha\beta}(\omega, \mathbf{q}) = \frac{2}{(2\pi\hbar)^3} \oint \frac{\mathrm{d}S_k}{v}\, \gamma_{\alpha\beta}(\mathbf{k}, \omega, \mathbf{q})|^2\, \mathrm{Im}\, \frac{q_n^2 v_n^2}{q_n^2 v_n^2 - \omega^2 - i2\omega\Gamma}\,, \tag{5}$$

where the Cartesian component n is chosen along the normal to the surface and the integration is performed over the Fermi surface. When the frequency of the exciting light is smaller than the energies of transitions between energy bands (interband transitions), the Raman vertex $\gamma_{\alpha\beta}(\mathbf{k}, \omega, \mathbf{q})$ is related to the reciprocal effective-electron-mass tensor, whereby the screening of the external force acting on the electrons must be taken into account [2, 3, 10, 17]

$$\gamma_{\alpha\beta}(\mathbf{k}, \omega, \mathbf{q}) = \mu_{\alpha\beta}(\mathbf{k}) - \oint \frac{\mathrm{d}S_k}{v}\, \mu_{\alpha\beta}(\mathbf{k})\, \frac{q_n v_n}{q_n v_n - \omega - i\Gamma} \left(\oint \frac{\mathrm{d}S_k}{v}\, \frac{q_n v_n}{q_n v_n - \omega - i\Gamma}\right)^{-1}. \tag{6}$$

We recall that the measurements were performed with the laser lines in the visible range in which strong interband excitations take place [23], and therefore the Raman vertex is expected to become resonant. Actually, the experimental data shown a sharp increase of the absolute electronic scattering efficiency by a factor of four above the laser energy of 1.8 eV (Fig. 4b). The efficiency for phonon scattering increases by a

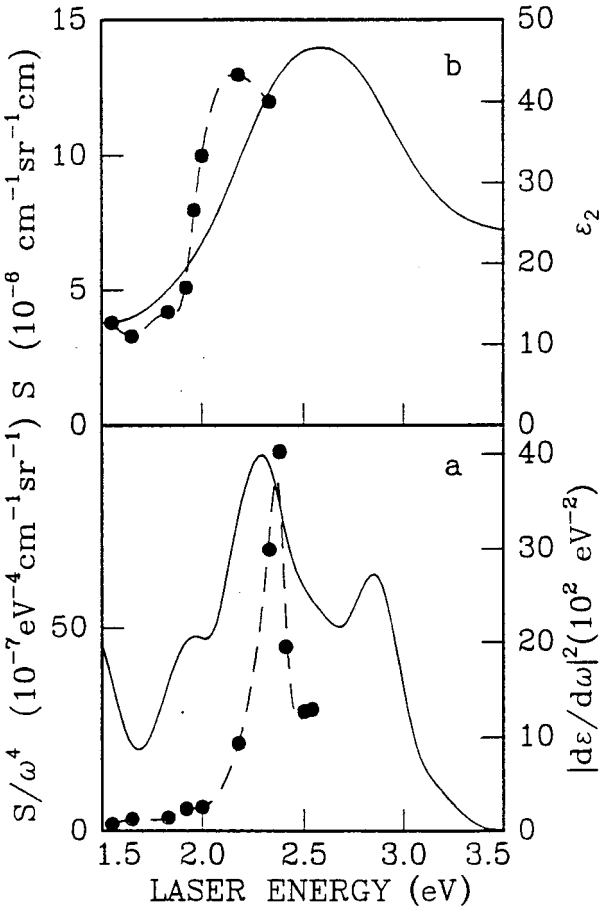

Fig. 4. Absolute Raman efficiencies for a) phonon and b) electronic scattering in OS measured at 10 K (dots, the dashed line are just guides to the eye). The solid lines display the imaginary part ε_2 of the dielectric function [23] (compared to the electronic scattering resonance) and the value of $|d\varepsilon/d\omega|^2$, often used to describe phonon resonances in semiconductors, the latter appropriately rescaled so as to match the measured absolute scattering efficiencies

factor 100, showing a narrow peak near 2.38 eV (Fig. 4a). The absolute efficiencies were determined experimentally [25] correcting for the complex refractive index [26] and comparing the measured intensities with an SrF_2 standard [25]. These facts provide evidence for strong resonant contributions to the Raman scattering efficiencies of Os which are related to the strong increase of the interband absorption peak near 2.5 eV [23]. Nevertheless, in view of the above-mentioned weak experimental variation of the polarization and momentum dependent anisotropy of the electronic scattering on laser frequency and for the sake of computational ease, we stick in the following simulations of electronic Raman spectra to the effective-mass approximation.

The exponentially decaying light wave in a metal can be decomposed into a superposition of plane waves with a range of wave vectors **q**. Thus, the effective scattering efficiency becomes proportional to a convolution of the susceptibility $W(\omega, \mathbf{q})$ and the electromagnetic energy distribution in the metal $F(q, q_0)$,

$$\frac{d^2S}{d\omega\, d\Omega}(\omega, q_0) \sim \int_{-\infty}^{\infty} W(\omega, q)\, F(q, q_0)\, dq\,. \tag{7}$$

Following [27] we take $F(q,\, q_0)$ to have the form

$$F(q,\, q_0) \simeq \frac{4A(Q)\, q^2}{|Q^2 - q^2|^2}\,. \tag{8}$$

Equation (8) respresents a skew lineshape with a peak position $q_0 = |Q| = 4\pi \times \sqrt{n^2 + k^2}/\lambda$, a width (FWHM) $\Delta q = 8\pi k/\lambda$. $A(Q)$ is a parameter independent of q while n and k are the real and imaginary parts of the complex refractive index at the laser wavelength (in vacuum) λ.

According to energy band structure calculations [28, 29], the compensated 5d transition metal Os has a FS consisting of four 4 sheets: U7h, KM8h, Γ9e and Γ10e. In this notation the position of the center of the surface (or the open direction in the case of an open surface), the band in which it lies, and its electron or hole character are specified. In our calculations we confined ourselves to two main electron sheets Γ9e and Γ10e, which are similar in form and close in dimensions and contribute considerably to the density of states (more than half of the total) at the Fermi surface. We performed numerical calculations aiming at investigating the effect of the FS sheet anisotropy on the frequency dependences of the **q**-dependent electronic Raman scattering and estimating the value of intersheet mass fluctuations. In order to model these sheets we used a second-nearest-neighbor tight-binding expression [8] for $E(\mathbf{k})$ obtained by neglecting basal plane anisotropy,

$$E(\mathbf{k}) = E_1(\cos a\varkappa + D_z \cos ck_z + D_2 \cos a\varkappa \cos ck_z)\,, \tag{9}$$

where a and c are lattice constants, $\varkappa = \sqrt{k_x^2 + k_y^2}$ is the electron wave vector component in the basal plane, E_1, D_z and D_2 are energy band parameters. The model FS $E(\mathbf{k}) = E_1 D_\mathrm{f}$ (insert in Fig. 2) is a surface of rotation about the AΓ direction with the curvature determined by the parameters D_z and D_2. The parameters $D_\mathrm{f} = -0.1$, $D_z = 0.7$, $D_2 = 1.5$ for the first sheet and $D_\mathrm{f} = -0,1$, $D_z = 0.6$, $D_2 = 2.5$ for the second one were chosen so as to simultaneously fit approximately the axis dimensions of the two electron sheets Γ9e and Γ10e [28]. The ratio of the maximum electron velocities for two perpendicular **q**-directions (along the c-axis and in the basal plane) was estimated from the observed ratio of the peak positions in electronic light scattering spectra (Fig. 1) which coincides with the ratio of the **q**-positions of the phonon anomalies (Fig. 3) for those directions. This resulted in a maximum velocity along the c-axis approximately 20% larger than that for in-plane directions. Adjusting the parameter E_1 which determines the magnitudes of the velocities to ≈400 meV, we fitted the spectrum calculated for the smallest experimental excitation energy $\lambda = 7500\,\text{Å}$ and in-plane probed wave vector to the measured one, using a constant $\Gamma = 10\,\mathrm{cm}^{-1}$. From this fit an estimate of (3 to 5) $\times 10^7$ cm/s for the electron velocity was extracted. The obtained value of the E_1 parameter was then used to calculate the electronic Raman continua for different directions and magnitudes of the probed wave vectors.

The experimental and calculated dependences of the peak energy on **q** are shown in Fig. 2. Good agreement is found in the range of small q-values $< 10^6\,\mathrm{cm}^{-1}$). However, for large q the experimental data lie well above the calculated ones. The broadening of the peaks at large wave vectors is also larger than the theory predicts. The spectra measured with $\lambda = 6471\,\text{Å}$ are displayed in Fig. 5 together with those calculated including both FS sheets. A large discrepancy in the frequency of the maximum in the spectra is found for **q** along the c-axis (the same discrepancy is found for the calculation per-

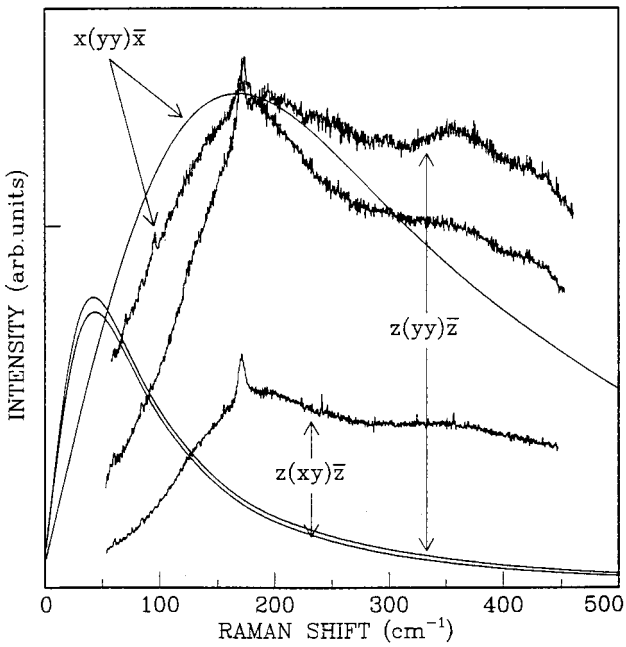

Fig. 5. Measured and calculated (using the effective mass approximation with the band parameters employed in the calculation of Fig. 2, solid lines) electronic Raman spectra for different polarization geometries. $\lambda = 6471$ Å ($q = 10.1 \times 10^5$ cm^{-1}). Both Γ9e and Γ10e sheets were used in this calculation

formed with only one sheet) which remains for different FS curvatures (different D_i), although the discrepancies in peak positions decrease when going to a more 'spherical' Fermi surface. Since the Raman vertex we have used for the electronic excitations enhances the contributions of FS regions with large curvature in the integral of Eqn. (5), it is unreasonable to expect a close coincidence of the peak energies for two mutually perpendicular **q**-directions. A large curvature is found in these FS regions where transition from the top (or the bottom) of the surface to its lateral part occur (e.g. in ΓL direction, see insert in Fig. 2). The projection of the Fermi velocity along z in the range of large curvature is much smaller than its in-plane component, a fact that explains the obtained result.

According to the results of calculations which included only the Γ9e sheet the $z(yy)\,\bar{z}$ intensity should equal that for $z(xy)\,\bar{z}$ polarization. In view of the form of the E_{2g} Raman tensor, which corresponds to a diagonal but traceless matrix, this implies a full screening of the A_{1g} scattering for **q** along the c-axis. In our measurements, however, the A_{1g} component has a higher intensity than the E_{2g} component (Fig. 5). Taking both Γ9e and Γ10e sheets into account in the calculation leads to the appearance of the A_{1g} continuum arising from intersheet mass fluctuations. However, the strength of the calculated A_{1g} component with $\mathbf{q} \parallel \hat{\mathbf{c}}$ remains negligibly small (Fig. 5, difference between $z(xy)\,\bar{z}$ curve and $z(yy)\,\bar{z}$ curve). It should be noted that the calculated absolute cross-sections for $A_{1g}(xx)$ ($\mathbf{q} \parallel \hat{\mathbf{c}}$) were found to be two orders of magnitude smaller than the measured ones at the resonance tail ($E_{ex} < 1.7$ eV). Although the inclusion of other

sheets of the FS may enhance the screened scattering of $A_{1g}(xx)$ ($\mathbf{q} \parallel \hat{\mathbf{c}}$) symmetry [6], it does not seem possible to change the results radically by including such sheets in the calculation. On the other hand, the calculated spectrum for $A_{1g}(zz)$ ($\mathbf{q} \perp \hat{\mathbf{c}}$) polarization is rather intense, while the measured one is negligible (not shown) [30].

5. Conclusions

The results obtained show that electronic light scattering in Os cannot be described within the standard **q**-dependent theory which relates it to mass fluctuations using only an average of the *two* main FS sheets of Os. As already mentioned, strong resonant effects have been found in the Raman efficiencies of Os which occur at exciting laser frequencies corresponding to strong interband absorption peaked near 2.5 eV (Fig. 4a, b). We note that, although the location of the measured phonon resonance is close to a feature calculated in $|\mathrm{d}\varepsilon/\mathrm{d}\omega|^2$, the former is rather narrow in comparison with the latter. This may be an indication of different response (or nonconstant deformation potential) of the electron bands over the Brillouin zone to the lattice vibration. The same should be expected for electronic scattering because of the larger number of electron bands involved and a complicated dependence on **k** of the interband optical matrix elements. The resonant effects, perhaps, may substantially change the **k**-dependence of the Raman vertex over the FS and cannot be reduced to a simple multiplication of Eqn. (5) by a resonant coefficient.

The dominant mechanism which determines electronic scattering around the FS, although not yet quantitatively clear, should also determine the effects observed in the self-energies of optical phonons. As for the observed correlation of the **q**-dependences in electronic Raman scattering and phonon self-energy it is difficult to expect a similarity of the **k**-dependences of an electron–phonon coupling (including the states near the Fermi level) and the resonant Raman vertex defined by the transition from (or to) the bands lying far from the Fermi level. The frequency shift and the width induced in the phonon by electron–phonon coupling are described by a complex self-energy $\Sigma(\omega, \mathbf{q})$ which is given by an equation similar to (5) [16], including both the real and the imaginary parts of the polarization operator with $\gamma^2_{\alpha\beta}(\mathbf{k})$ replaced by the squared electron–phonon vertex, and with the scattering frequency ω replaced by the phonon frequency. The close correlation of the **q**-dependences in electronic Raman scattering and phonon self-energy is, most probably, due to ($\mathbf{k}$, $\mathbf{q}$)-dependent singularities in the polarization operator (density–density response function).

It is known that the strong phonon anomalies found in h.c.p. transition metals near the zone center can be reproduced using phenomenological charge-fluctuation models [31, 32]. These findings imply that dynamic charge density waves, induced by the phonons of specific symmetry, are the source of the ($\mathbf{k}$, $\mathbf{q}$)-dependent anomalies in the renormalized electronic response. Similar singularities, localized in specific regions of the Brillouin zone, may determine the spatial dispersion of both the electronic continua and the phonon self-energies, since both phenomena are affected by electron–phonon coupling. Resonant terms, which have been found to affect the Raman vertices are also able to select contributions from certain regions of wave vector space when a value of an anomalous **q**-vector and a frequency of the interband transitions, probing the Fermi level in this **k**-region, are simultaneously satisfied at the exciting laser energy. The following facts also support the picture given above. Although our experimental data

show the existence of similar **q**-dependent anomalies in the phonon self-energy of the electronic analog of osmium, the 5d metal ruthenium, no clear dependence of the electronic continua was observed for the wave vectors investigated in Ru; only a rather strong flat background appeared [33]. This fact may be attributed to the lack of interband transitions at the Fermi level in the **k**-region where electronic excitations strongly interacting with phonons dominate, in contrast to the case of Os.

Finally, we return to the behaviour of the longitudinal phonon having a **q**-direction along $[10\bar{1}0]$. This mode, in contrast to two transverse vibratrions with **q** along [0001] and $[1\bar{2}10]$, contains a fully-symmetric (A_{1g}) component within the group of the **q**-vector and exhibits a supression of both the anomalous dispersion and the Landau damping (Fig. 3). At the same time, the electronic excitation continua which have been assumed to be the cause of the phonon anomalies, were observed in the *xx* and *yy* polarization geometries (corresponding **q**-directions $[10\bar{1}0]$ and $[1\bar{2}10]$) with approximately the same lineshapes and intensities (Fig. 1). This contradiction may be attributed to screening effects reducing the electron–phonon coupling for the longitudinal phonon. It may be correlated with the weak anisotropy of electron–phonon coupling over the **k**-region around a singularity in the electron response. In contrast, the strong **k**-dependence of the resonant Raman vertex in this region may provide strong (i.e., only partially screened) A_{1g} electronic scattering.

In summary, we have presented the first (to our knowledge) experimental evidence of **q**-dependent optical phonon self-energies and of the electronic continuum observed by Raman scattering in a h.c.p. transition metal (osmium). An estimate of (3 to 5) $\times 10^7$ cm/s for the velocity of the electrons which strongly interact with the phonons was obtained. Calculations of the electronic light scattering were performed in the **q**-conserving regime with model energy bands which reproduce the main sheets of the Os FS. The results suggest a significant role of the resonant terms in the Raman vertex and the impossibility to explain the observed phenomena on the basis of the susceptibility of the noninteracting electrons. To clarify the origin of the electronic excitations and electron–phonon coupling under study the calculations of the resonant Raman scattering by electrons as well as phonon self-energies on the basis of a more realistic energy band structure, including electron self-energy renormalization [12, 34 to 36], are necessary.

After this manuscript was submitted a paper appeared dealing with vertex and renormalization corrections to the theory of the phonon self-energies (and, by extension, to that of the electronic scattering) [37], where the authors show that such corrections are negligible in the weak coupling regime. In this regime, the theory (Fig. 1a of [37])] is equivalent to that used in the present paper. While Eqn. (16) of [37] is able to account for an increase in phonon frequency with increasing **q** as observed in Fig. 3 for $\mathbf{q} \parallel [1\bar{2}10]$, it does not yield any contribution to the imaginary part of the self-energy and its **q**-dependence (i.e., the phonon width also displayed in Fig. 3). We are thankful to the authors of [37] for sending us a copy of their paper.

Acknowledgements The authors would like to thank G. P. Kovtun and V. A. Elenskii for the high-quality Os samples, H. Hirt, M. Siemers, P. Wurster and V. E. Mogilenskii for technical help. We dedicate this paper to the memory of Peter Wurster. This work was supported in part by ISF and RF government grants No. NMF000 and NMF300. Yu. S. Ponosov acknowledges useful conservations with E. G. Maksimov and E. Ya. Sherman and thanks DAAD for support.

References

[1] A. A. Abrikosov and L. A. Falkovskii, Zh. Eksper. Teor. Fiz. **40**, 262 (1961) (Soviet Phys. – J. Exper. Theor. Phys. **13**, 179 (1961)).
[2] A. A. Abrikosov and V. M. Genkin, Zh. Eksper. Teor. Fiz. **65**, 842 (1973) (Soviet Phys. – J. Exper. Theor. Phys. **38**. 417 (1974)).
[3] M. V. Klein and S. B. Dierker, Phys. Rev. B **29**, 4976 (1984).
[4] S. L. Cooper and M. V. Klein, Comments Cond. Mat. Phys. **15**, 19 (1990).
[5] A. Zawadowski and M. Cardona, Phys. Rev. B **42**, 10732 (1990).
[6] M. Krantz, I. I. Mazin, D. H. Leach, W. Y. Lee, and M. Cardona, Phys. Rev. B **51**, 5949 (1995).
[7] T. Devereaux and D. Einzel, Phys. Rev. B **51**, 16336 (1995).
[8] X. K. Chen, J. C. Jrwin, R. Liang, and W. N. Hardy, Physica **227C**, 113 (1994).
[9] C. Thomsen, in: Light Scattering in Solids VI, Eds. M. Cardona and G. Güntherodt, Springer-Verlag, Berlin 1991, (p. 285).
[10] M. Cardona and I. Ipatova, in: Elementary Excitations in Solids, Eds. J. L. Birman, C. Sebenne, and R. F. Wallis, North-Holland Publ. Co., Amsterdam 1992 (p. 237).
[11] K. Itai, Phys. Rev. B **45**, 707 (1992).
[12] S. N. Rashkeev and G. Wendin, Phys. Rev. B **47**, 11603 (1993); Z. Phys. B **93**, 33 (1993).
[13] B. Friedl, C. Thomsen, H.-U. Habermeier, and M. Cardona, Solid State Commun. **81**, 989 (1992).
[14] D. Olego and M. Cardona, Phys. Rev. B **23**, 6592 (1981).
[15] Yu. S. Ponosov and G. A. Bolotin, Soviet Phys. – Solid State **27**, 1581 (1985).
[16] I. P. Ipatova and A. V. Subashiev, Zh. Eksper. Teor. Fiz. **66**, 722 (1974) (Soviet Phys. – J. Exper. Theor. Phys. **39**, 349 (1974)).
[17] I. P. Ipatova, M. I. Kaganov, and A. V. Subashiev, Zh. Eksper. teor. Fiz. **84**, 1830 (1983) (Soviet Phys. – J. Exper. Theor. Phys. **57**, 1066 (1983)).
[18] L. A. Falkovskii, Zh. Eksper. Teor. Fiz. **95**, 1145 (1989) (Soviet phys. – J. Exper. Theor. Phys. **68**, 661 (1989)).
[19] L. A. Falkovskii, Zh. Eksper. Teor. Fiz. **103**, 666 (1993).
[20] O. V. Misochko and E. Ya. Sherman, Phys. Rev. B. **51** (1995).
[21] G. Contreras, A. K. Sood, and M. Cardona, Phys. Rev. B **32**, 930 (1985).
[22] I. P. Ipatova, A. V. Subashiev, and V. A. Shchukin, Fiz. Tverd. Tela **24**, 3401 (1982) (Soviet Phys. – Solid State **24**, 1932 (1982)).
[23] V. V. Nemoshkalenko et al., Soviet Phys. – J. Exper. Theor. Phys. **20**, 201 (1986).
[24] M. V. Klein, in: Light Scattering in Solids, Eds. M. Cardona and G. Güntherodt, Springer-Verlag 1975 (p. 174).
[25] J. M. Calleja, H. Vogt, and M. Cardona, Phil. Mag. **A45**, 239 (1982).
[26] M. V. Klein, J. A. Holly, and W. S. Williams, Phys. Rev. B **17**, 1546 (1978).
[27] A. Dervisch and R. Loudon, J. Phys. C **9**, L669 (1976).
[28] O. Jepsen, O. K. Andersen, and A. R. Mackintosh, Phys. Rev. B **12**, 3084 (1975).
[29] V. N. Antonov, A. I. Baglyuk, A. Ya. Petrov et al., Fiz. Nizk. Temp. **19**, 786 (1993) Soviet Phys. – Low-Temp. Phys. **19**, 561 (1993)).
[30] Yu. S. Ponosov, C. Thomsen, and M. Cardona, Physica **235/240C**, 1153 (1994).
[31] N. Wakabayashi, Comments Solid State Phys. **10**, 11 (1981).
[32] N. Wakabayashi, R. H. Sherm, and H. G. Smith, Phys. Rev. B **25**, 5122 (1982).
[33] Yu. S. Ponosov et al., to be published.
[34] S. V. Shulga, O. V. Dolgov, and E. G. Maksimov, Physica **178C**, 317 (1990).
[35] S. V. Shulga and E. G. Maksimov, Solid State Commun. **97**, 553 (1996).
[36] B. N. Kostur and G. M. Eliashberg, Soviet Phys. – J. Exper. Theor. Phys. Lett. **53**, 39 (1991).
[37] A. S. Alexandrov and J. R. Schrieffer, Phys. Rev. B **56**, 13731 (1997).